Electronic Supplementary Material (ESI) for New Journal of Chemistry.

Hybrid shells of N-doped carbon encapsulated by MnO nanoparticles towards oxygen reduction reaction electrocatalysts

Yanan Li, Jie Han,* Zhilong Xu, Rong Guo*

School of Chemistry and Chemical Engineering, Yangzhou University, Yangzhou,

Jiangsu, 225002, P. R. China. E-mail: hanjie@yzu.edu.cn; guorong@yzu.edu.cn

Electrochemical Test

To prepare the working electrode, 3.5 mg of catalyst mixed with 1.5 mg Cabot Vulcan XC-72 carbon (Vc-72) were dispersed in a solution containing 500 μL of mixed solution (2-propanol mixed with water (V_{C3H8O}:V_{H2O}=1:1) and 0.5 wt % Nafion solution). The suspension was ultrasonically dispersed to form a homogeneous ink. After that, the ink was pipetted onto the GC electrode and then was naturally drying to form a thin catalyst layer on the GC electrode.

The tests were conducted on a computer-controlled potentionstat/galvanostat workstation at room temperature. The supporting electrolyte was 0.1 mol L^{-1} KOH aqueous solution, which was purged with N_2 or O_2 (purity 99.995%) for at least 30 min prior to testing and maintained under N_2 or O_2 atmosphere during the test. Cyclic voltammograms were recorded from 0.2 to -0.8 V *versus* Ag/AgCl in N_2- and O_2-staurated 0.1 mol L^{-1} KOH electrolyte solutions with a scan rate of 20 mV s^{-1}. Rotating disk electrode (RDE) was performed in O_2-staurated 0.1 mol L^{-1} KOH at 1600 rpm with a sweep rate of 5 mV s^{-1}. All potentials were reported with reference to the reversible hydrogen electrode (RHE) potential scale. In 0.1 mol L^{-1} KOH solution, the potential of Ag/AgCl was calibrated as +0.965 V with respect to RHE.

Koutecky-Levich (K-L) plots was analyzed at various electrode potentials. The K–L plots show linear relationships between j_k^{-1} and $\omega^{-1/2}$, the higher the slope is the smaller the number of electron transfer and the lower the oxygen reduction electric catalytic activity. The slopes of their best linear fit lines were used to calculate the electron transfer number (n) according to the K-L equation:

$$\frac{1}{J}=\frac{1}{J_L}+\frac{1}{J_K}=\frac{1}{B\omega^{\frac{1}{2}}}+\frac{1}{J_K} \tag{1}$$

$$B=0.62nFC_0(D_0)^{2/3}v^{-1/6} \tag{2}$$

$$J_K=nFkC_0 \tag{3}$$

where J is the measured current density, J_K and J_L are the kinetic- and diffusion-limiting current densities, ω is the angular velocity, n represents the overall number of electrons transferred in oxygen reduction, F is the Faraday constant, C_0 is the bulk concentration of O_2, D_0 is the diffusion coefficient of O_2 in 0.1 mol L^{-1} KOH electrolyte, v is the kinematic viscosity of the electrolyte and k is the electron transfer rate constant.

The ring electrode can detect the intermediate product hydrogen peroxide produced by the ORR catalysts on the disk electrode, and the percent content of hydrogen peroxide (y_{peroxide}) is the ratio of the amount of hydrogen peroxide generated in the ORR total product. On account of the disk current (i_d) and ring current (i_r), the y_{peroxide} and electron transfer number (n) c an be calculated based on the following equations:

$$y_{\text{peroxide}}=200i_r/(Ni_d+i_r) \tag{4}$$

$$n=4Ni_d/(Ni_d+i_r) \tag{5}$$

where N is the current collection efficiency of RRDE. N was determined to be 0.37.

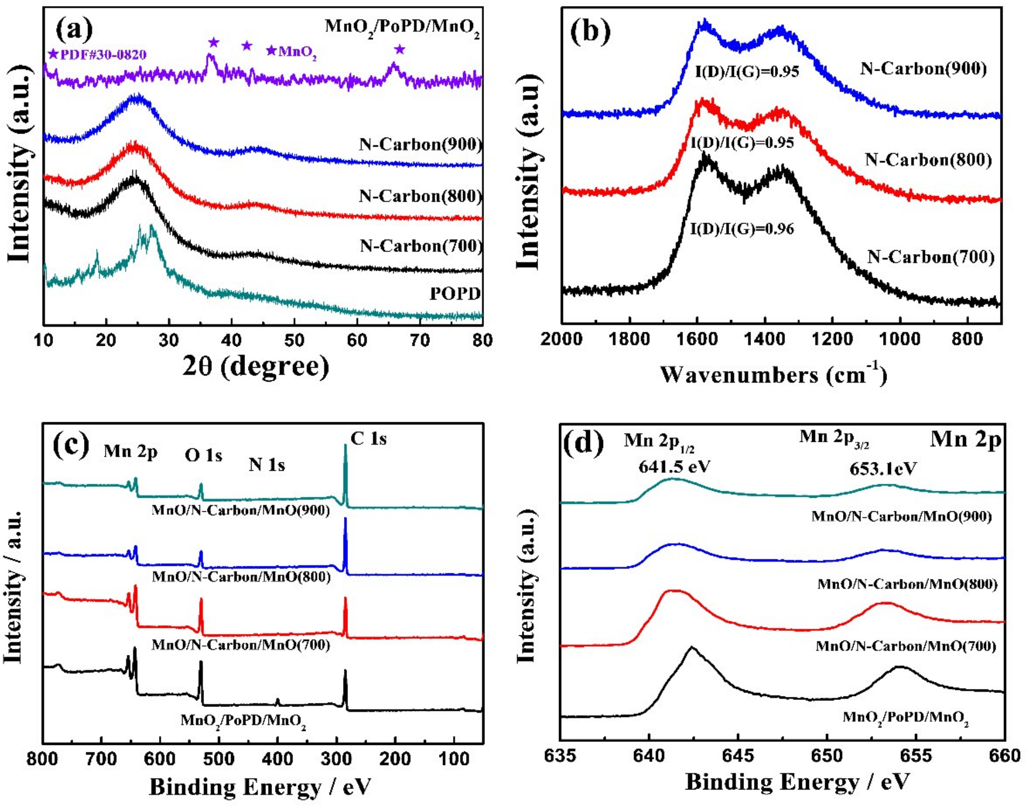
(a)
MnO$_2$/PoPD/MnO$_2$
★PDF#30-0820
★MnO$_2$
N-Carbon(900)
N-Carbon(800)
N-Carbon(700)
POPD
Intensity (a.u.)
2θ (degree)
10 20 30 40 50 60 70 80
(b)
I(D)/I(G)=0.95
N-Carbon(900)
I(D)/I(G)=0.95
N-Carbon(800)
I(D)/I(G)=0.96
N-Carbon(700)
Intensity (a.u)
Wavenumbers (cm^{-1})
2000 1800 1600 1400 1200 1000 800
(c)
Mn 2p
O 1s
N 1s
C 1s
MnO/N-Carbon/MnO(900)
MnO/N-Carbon/MnO(800)
MnO/N-Carbon/MnO(700)
MnO$_2$/PoPD/MnO$_2$
Intensity / a.u.
Binding Energy / eV
800 700 600 500 400 300 200 100
(d)
Mn 2p$_{1/2}$
641.5 eV
Mn 2p$_{3/2}$
653.1eV
Mn 2p
MnO/N-Carbon/MnO(900)
MnO/N-Carbon/MnO(800)
MnO/N-Carbon/MnO(700)
MnO$_2$/PoPD/MnO$_2$
Intensity (a.u.)
Binding Energy / eV
635 640 645 650 655 660

Fig. S1 (a) XRD patterns of PoPD, N-Carbon and MnO_2/PoPD/MnO_2 hybrid shells, (b) Raman spectra of N-Carbon, (c) XPS spectra and (d) XPS spectra of Mn 2p of MnO_2/PoPD/MnO_2 and MnO/N-Carbon/MnO hybrid shells.

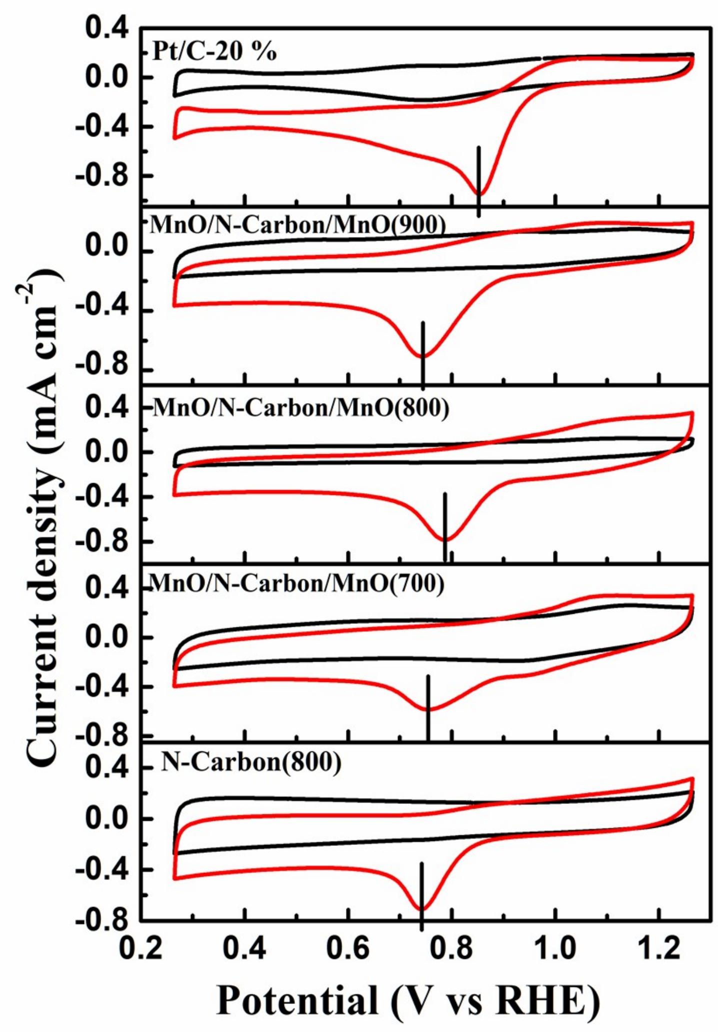

Fig. S2 CV curves of N-Carbon(800), MnO/N-Carbon/MnO and Pt/C catalyst in 0.1 M KOH saturated with N_2 (black solid curves) or O_2 (red solid curves).

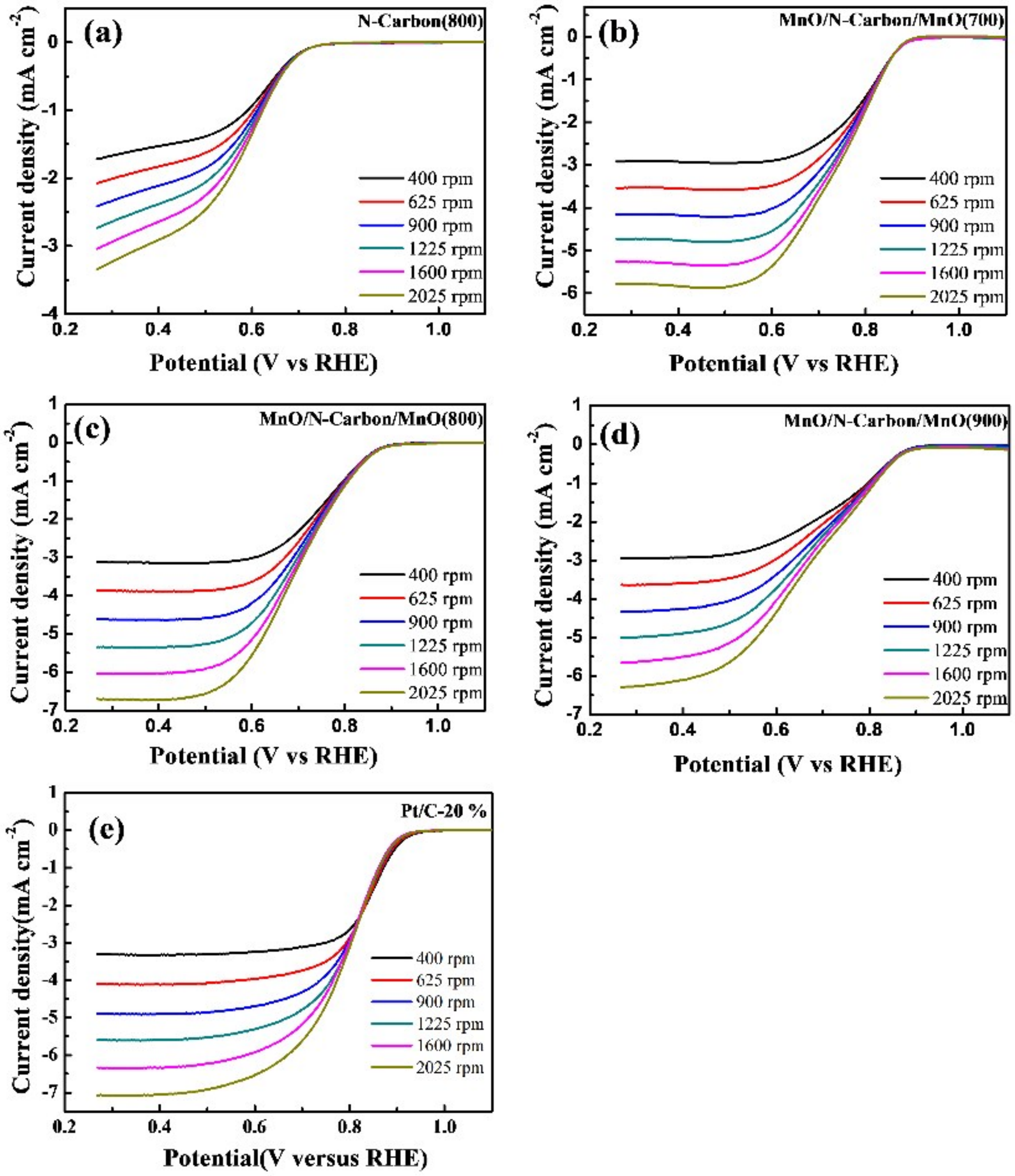

Fig. S3 LSV curves of (a) N-Carbon(800), (b) MnO/N-Carbon/MnO(700), (c) MnO/N-Carbon/MnO(800), (d) MnO/N-Carbon/MnO(900) and (e) Pt/C in O_2-saturated 0.1 M KOH with various rotating speeds.

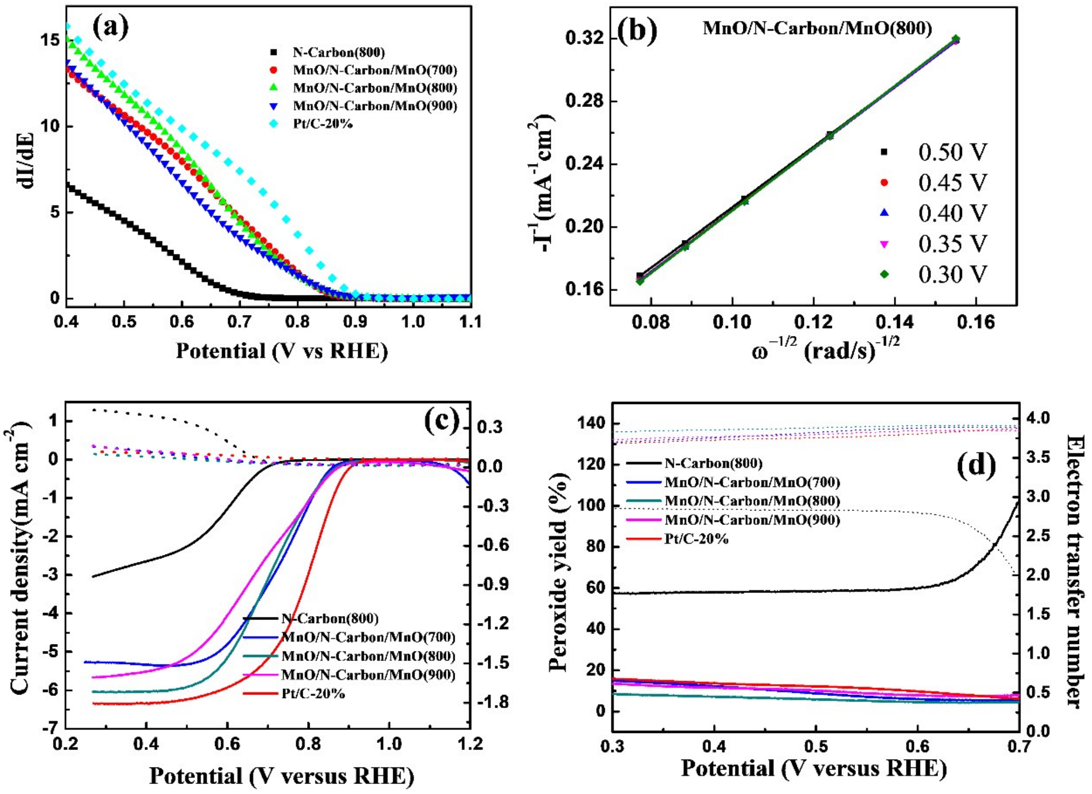

Fig. S4 (a) The differential plots of *I* versus *E* constructed from the LSV curve. From the sharply increased slope of the plots, the onset potential indicative of the start of the ORR can be clearly seen. (b) K-L plots of MnO/N-Carbon/MnO(800) at 0.3-0.5 V. (c) The polarization curves of different catalysts and Pt/C recorded on disk (solid line) and the ring (dotted line). (d) Peroxide yield (solid line) and the electron transfer number (dotted line) of different catalysts and Pt/C at different potentials.

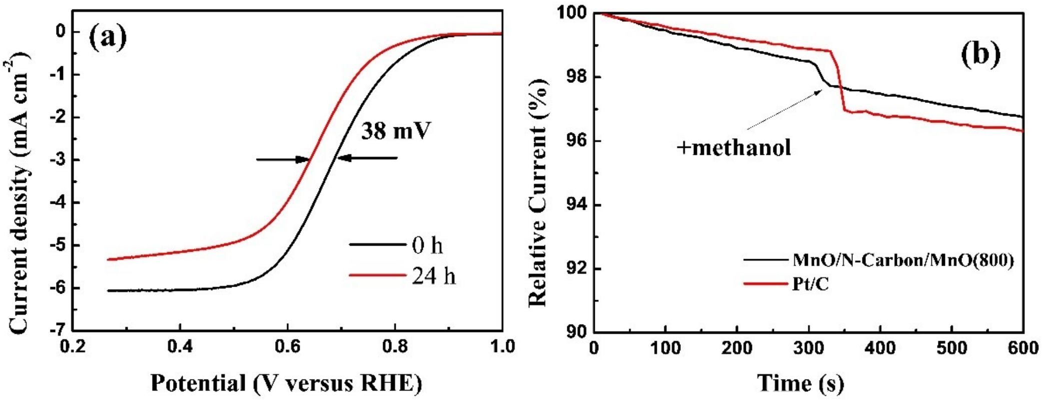

Fig. S5 (a) The stability tests for ORR of MnO/N-Carbon/MnO(800) and Pt/C in O_2-saturated 0.1 KOH. (b) Chronoamperometric curves of MnO/N-Carbon/MnO(800) and Pt/C maintained at 0.8 V in O_2-saturated 0.1 M KOH with 3 M methanol (the arrow indicates the addition of 3 M methanol into the electrochemical cell).

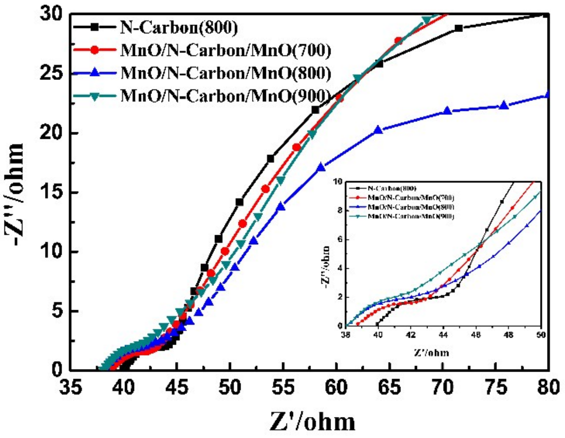

Fig. S6 Nyquist plots of N-Carbon(800) and MnO/ N-Carbon/MnO hybrid shell in 0.1 mol L^{-1} KOH.

Table S1 Comparison of the electrochemical performances of MnO/ N-Carbon /MnO(800) hybrid shells involved in ORR with reported results.

Catalyst	Morphology	E_{onset} (V)	I_s (mA cm^{-2})	*n*	Reference
MnO	Nanorods	-	0.85	2.19	1
N/C-G-MnO	-	-	3.75	3.98	2
3D-N-RGO/MnO	Nanoparticles	0.83	1.62	3.03	3
MnO/RGO	Octahedral	-	4.72	3.85	4
GNS@MnO@N-doped carbon	Nanoparticles	0.98	5.10	3.08	5
MnO/NG-900	Nanoparticles	0.89	4.17	3.70	6
MnO/ N-Carbon /MnO(800)	Sandwich-like hybird shells	0.91	6.01	3.93	this work

References

1 X. Wu, X. Gao, L. Xu, T. Huang, J. Yu, C. Wen, Z. Chen, J. Han, *Int. J. Hydrogen Energy,* 2016, **41**, 16087-16093.

2 B. Wang, S. Pan, Y. Qin, W. Tan, Y. Tao, K. Li, Y. Kong, *Synth. Met*, 2017, **224**, 92–98.

3 R. Chen, J. Yan, Y. Liu, J. Li, *J. Phys. Chem. C.,* 2015, **119**, 8032-8037.

4 Q. Wu, M. Jiang, X. Zhang, J. Cai, S. Lin, *J. Mater Sci.*, 2017, **52**, 6656-6669.

5 Y. Wang, X. Ding, F. Wang, J. Li, S. Song, H. Zhang, *Chem. Sci.*, 2016, **7**, 4284–4290.

6 A. Arunchander, M. Vivekanantha, S. Gouse Peeraa, A. K. Sahu, *RSC Adv.*, 2016, **6**, 95590–95600.